

Wnt11 Functions in Gastrulation by Controlling Cell Cohesion through Rab5c and E-Cadherin

Florian Ulrich,^{1,3,5} Michael Krieg,^{2,4,5}
Eva-Maria Schötz,^{1,3,5} Vinzenz Link,^{1,3}
Irinka Castanon,^{1,3} Viktor Schnabel,^{1,3}
Anna Taubenberger,^{2,4} Daniel Mueller,^{2,4}
Pierre-Henri Puech,^{2,4}
and Carl-Philipp Heisenberg^{1,3,*}

¹Max Planck Institute of Molecular Cell Biology
and Genetics

Pfotenhauerstr. 108
01307 Dresden
Germany

²Center of Biotechnology
Technische Universität Dresden
Cellular Machines
Tatzberg 49
01307 Dresden
Germany

Summary

Wnt11 plays a central role in tissue morphogenesis during vertebrate gastrulation, but the molecular and cellular mechanisms by which Wnt11 exerts its effects remain poorly understood. Here, we show that Wnt11 functions during zebrafish gastrulation by regulating the cohesion of mesodermal and endodermal (mesendodermal) progenitor cells. Importantly, we demonstrate that Wnt11 activity in this process is mediated by the GTPase Rab5, a key regulator of early endocytosis, as blocking Rab5c activity in wild-type embryos phenocopies *slb/wnt11* mutants, and enhancing Rab5c activity in *slb/wnt11* mutant embryos rescues the mutant phenotype. In addition, we find that Wnt11 and Rab5c control the endocytosis of E-cadherin and are required in mesendodermal cells for E-cadherin-mediated cell cohesion. Together, our results suggest that Wnt11 controls tissue morphogenesis by modulating E-cadherin-mediated cell cohesion through Rab5c, a novel mechanism of Wnt signaling in gastrulation.

Introduction

During vertebrate gastrulation, a tightly coordinated series of cellular movements organizes the three germ layers: ectoderm, mesoderm, and endoderm (Stern, 2004). In zebrafish, gastrulation starts with the internalization of mesodermal and endodermal (mesendodermal) progenitors at the blastoderm margin (Montero et al., 2005; Warga and Kimmel, 1990). Mesendodermal progenitors that will give rise to prechordal plate, the anterior-most axial mesendoderm, internalize by syn-

chronized ingression of single cells at the dorsal side of the gastrula where the embryonic organizer (shield) forms. Once internalized, prechordal plate progenitors migrate as a cohesive group of cells away from the blastoderm margin toward the animal pole of the gastrula using the overlying noninternalizing ectodermal progenitor cell layer as a substrate (Montero et al., 2005).

Wnt11 plays a pivotal role in controlling prechordal plate progenitor cell movements, possibly by coordinating directed cell migration with cellular process orientation (Heisenberg et al., 2000; Ulrich et al., 2003). However, the molecular mechanisms by which Wnt11 signaling affects prechordal plate progenitor movements are still uncertain. Wnt11 signals through a pathway that shares several components with the *Drosophila* planar cell polarity (PCP) pathway, a known regulator of epithelial planar cell polarity (Tada et al., 2002; Veeman et al., 2003). In *Drosophila*, the polarized intracellular distribution of PCP components is thought to be a mechanism to directly determine cell polarity (Adler, 2002). In vertebrate gastrulating cells, no clear polarized distribution of any of the PCP components has yet been observed, suggesting that Wnt11 might employ other mechanisms (Tada et al., 2002; Veeman et al., 2003). Intriguingly, the Wnt11 receptor Frizzled-7 (Fz-7) (Djiane et al., 2000) is required for tissue separation during *Xenopus* gastrulation (Winklbauer et al., 2001), suggesting that Wnt signaling controls cell migration by modulating cell adhesion.

For cells to migrate, they have to dynamically modulate cell adhesion in order to build and break contacts during translocation (Lauffenburger and Horwitz, 1996). Both endocytosis and recycling of adhesion molecules have been suggested as efficient intracellular mechanisms for cells to remodel their adhesive contacts (Le et al., 1999). The GTPase Rab5 functions as a key component in the regulation of intracellular trafficking both at the level of receptor endocytosis and endosome dynamics (Zerial and McBride, 2001). Activating Rab5 in cell culture stimulates endocytosis and endosome motility and leads to disassembly of adherens junctions and increased cell migration (Murphy et al., 1996; Palacios et al., 2005; Spaargaren and Bos, 1999). These findings suggest a role for Rab5-mediated endocytosis in promoting cell motility.

The prechordal plate in zebrafish is formed by a highly cohesive group of axial mesendodermal progenitor cells that move in a straight path from the germ ring toward the animal pole of the gastrula (Ulrich et al., 2003). The dynamic modulation of cell adhesion is likely to be important for large-scale coordination of prechordal plate progenitor movement as it may allow cells to efficiently assemble into, as well as maintain, a cohesive tissue that shares common migratory properties. We recently found that E-cadherin-mediated cell cohesion—the ability of cells to aggregate into distinct clusters—is required for the coordinated movement of prechordal plate progenitor cells during zebrafish gastrulation (Montero et al., 2005). In this study, we address

*Correspondence: heisenberg@mpi-cbg.de

³Lab address: <http://www.mpi-cbg.de/research/groups/heisenberg/heisenberg.html>

⁴Lab address: <http://www.biotec.tu-dresden.de/mueller>

⁵These authors contributed equally to this work.

the role of Rab5c-mediated cell adhesion dynamics as one possible target mechanism by which Wnt11 controls mesendodermal cell cohesion and migration, and we present evidence for E-cadherin to function downstream of Wnt11 in this process.

Results

Wnt11-Dependent Control of Prechordal Plate Movement

In zebrafish *slb/wnt11* mutants, prechordal plate progenitors, once internalized, exhibit reduced movements from the axial germ ring (shield) toward the animal pole of the gastrula (Ulrich et al., 2003). To visualize where and when this movement phenotype arises, we recorded time lapse movies of cellular rearrangements within the shield of wild-type and *slb* mutant embryos beginning at the onset of gastrulation. In wild-type embryos, prechordal plate progenitors moved both toward the overlying epiblast cell layer and along it toward the animal pole (Figures 1A–1C; Movie S1). *slb* prechordal plate progenitors also moved normally toward the epiblast; however, in contrast to wild-type, the movement velocities toward the animal pole were slower and cells often moved in the opposite direction toward the vegetal pole (Figures 1D–1G and data not shown; Movie S2). This difference in animal pole-directed movement between wild-type and *slb/wnt11* mutant prechordal plate progenitors was independent of contact with the overlying epiblast (Figure 1H), suggesting that Wnt11 is equally required for the movement of cells within the forming prechordal plate and at the interface between prechordal plate and epiblast.

Prechordal plate progenitors assemble into a cohesive tissue within which the individual cells follow highly aligned movement tracks projecting toward the animal pole (Montero et al., 2003; Ulrich et al., 2003). To determine whether Wnt11 controls alignment of prechordal plate progenitor movement tracks relative to each other, we compared the “coherence” of cell movements at the leading edge of the forming prechordal plate from wild-type and *slb/wnt11* mutant embryos (Figures 1I and 1J). The coherence of prechordal plate progenitor cell movements at the onset of gastrulation was reduced in *slb/wnt11* mutant embryos compared to wild-type controls (Figure 1K). This suggests that Wnt11 is required to align the movement of individual prechordal plate progenitors and that this alignment might represent a way by which Wnt11 efficiently coordinates prechordal plate progenitor movement toward the animal pole.

Role of Wnt11 and E-Cadherin for Mesendodermal Cell Cohesion

The ability of prechordal plate progenitors to assemble into and persist as a cohesive tissue—via regulation of their adhesive properties—is likely to constitute an important mechanism by which individual cell movements within the prechordal plate are aligned. To examine whether Wnt11 might control alignment of prechordal plate progenitor movement by regulating the cohesion of these cells, we compared the aggregation behavior of wild-type versus *slb/wnt11* mutant mesendodermal

cells cultured on fibronectin (for details, see [Experimental Procedures](#)). During the first 6 hr in culture, nearly all wild-type mesendodermal cells formed both small (<10 cells) and large (>10 cells) confluent cell aggregates (Figures 2A and 2E). In comparable *slb/wnt11* mutant cell cultures, the relative amount of large aggregates was reduced, while the amount of small aggregates was significantly increased as compared to wild-type cultures ($p < 0.001$; Figures 2C and 2E). This suggests that Wnt11 is required for efficient cohesion of mesendodermal cells in culture.

We have previously shown that E-cadherin-mediated cohesion between mesendodermal cells is required for the movement and spreading of these cells during gastrulation (Montero et al., 2005). To test whether Wnt11 controls mesendodermal cell cohesion via E-cadherin, we compared the aggregation behavior of cultured wild-type versus *slb/wnt11* mutant cells when E-cadherin was knocked down in these cells (for details, see [Experimental Procedures](#)). While *slb/wnt11* mutant cells showed no significant differences in the distribution of small versus large confluent clusters when E-cadherin was knocked down ($p > 0.05$; Figures 2C–2E), wild-type cells displayed a significant increase in the fraction of small aggregates and a significant decrease in the relative amount of large clusters as compared to noninjected wild-type cells ($p < 0.05$; Figures 2A, 2B, and 2E). In contrast, binding of mesendodermal cells to their fibronectin substrate appeared to be not required for Wnt11-mediated mesendodermal cell aggregation (data not shown; Puech et al., 2005). These findings suggest that E-cadherin is involved in Wnt11-mediated mesendodermal cell cohesion.

To obtain insight into the cellular mechanisms that underlie Wnt11-mediated cohesion of mesendodermal cells, we analyzed the aggregation behavior of mesendodermal cells in culture using 4-D confocal microscopy. We observed that mesendodermal cells initially formed loosely associated spread out clusters of cells that, over a period of 60 min, transformed into confluent, rounded up cell aggregates (Figures 2F–2K). During this transformation process, mesendodermal cell aggregates reduced the outside surface area (1.4 times reduction for exemplary cluster shown in Figures 2F–2K) and, at the same time, strongly increased their cell-cell contact area (8.8 times increase for exemplary cluster shown in Figures 2F–2K; for details about cell surface and cell-cell contact area calculation, see [Supplemental Experimental Procedures](#)). This shows that the process of cell aggregation of mesendodermal cells involves highly dynamic changes in cell-cell contacts.

Wnt11-Mediated Changes in E-Cadherin Localization

To identify potential target molecules of Wnt11 function in modulating cell-cell contact dynamics, we compared the intracellular distribution of E-cadherin, a key regulator of cell-cell adhesion in zebrafish gastrulation (Babb and Marrs, 2004; Kane et al., 2005; Montero et al., 2005; Shimizu et al., 2005) in embryos mutant for *slb/wnt11* versus *slb/wnt11* mutant embryos, in which we expressed Wnt11 under the control of a heat-shock inducible promoter (*slb-hs-wnt11-HA* transgenic embryos). We used *slb-hs-wnt11-HA* transgenic and *slb/*

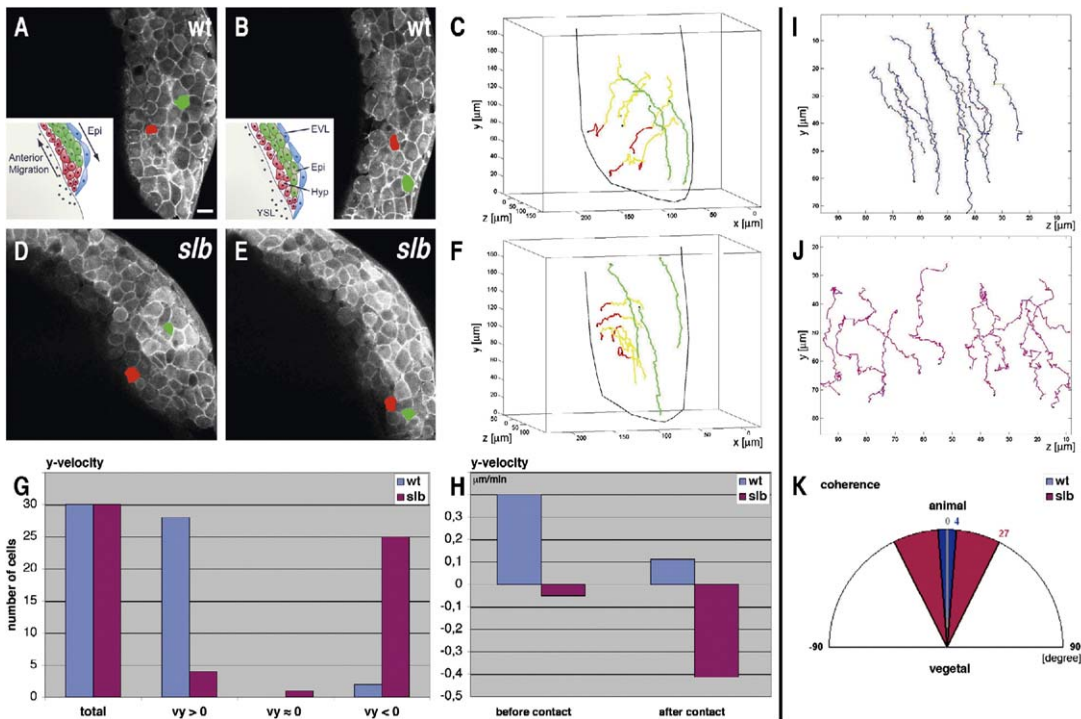


Figure 1. Cell Movements within the Axial Germ Ring (Shield) at the Onset of Gastrulation

(A, B, D, and E) Lateral views of the shield region of a wild-type (A and B) and *slb/wnt11* mutant embryo (D and E) at 60% epiboly (A and D) and 1.5 hr later (B and E). For the full sequence of images, see [Movies S1 and S2](#). Single hypoblast and epiblast cells were labeled in red and green, respectively. Epiblast and hypoblast cells were identified by their different net movement and cell morphology ([Montero et al., 2005](#)). Inlets in (A) and (B) show schematic representations of cell movements within the shield. EVL, enveloping layer; Epi, epiblast; Hyp, hypoblast; YSL, yolk syncytial layer. The scale bar represents 20 μm .

(C and F) Exemplary tracks of six hypoblast (red/yellow) and three epiblast cells (green) in a wild-type (C) and *slb/wnt11* mutant embryo (F) taken from the same movies as shown in (A), (B), (D), and (E) (see [Movies S1 and S2](#)). The red tracks delineate hypoblast cell movement before they reach the epiblast, while the yellow tracks demarcate the movement after contact with the epiblast. Black dots mark the starting points of the tracks. In total, 30 hypoblast and 10 epiblast cells from three embryos each were tracked in the wild-type and *slb/wnt11* mutant case.

(G) Distribution of average velocities in direction to the animal pole (v_y ; +y direction) between wild-type and *slb/wnt11* mutant prechordal plate progenitors.

(H) Average velocities in direction to the animal pole (v_y) in wild-type and *slb/wnt11* mutant prechordal plate progenitors before and after contact with the overlying epiblast cell layer.

(I and J) Exemplary track diagrams of progenitor cells at the leading edge of the prechordal plate from wild-type (I) and *slb/wnt11* mutants (J) shown in the y,z plane (for orientation, see [C] and [F]). Cells were tracked for 1 hr 30 min in 1 minute time intervals as described in [Montero et al. \(2003\)](#).

(K) Standard deviation (SD) of the net movement track directions of single progenitor cells at the leading edge of the prechordal plate from wild-type (blue) and *slb/wnt11* mutant embryos (red). High SD corresponds to low movement coherence and low SD to high coherence. All values in [degree] were normalized to the net movement direction of the prechordal plate (0 degree). For SD calculation, 40 cells from four embryos per genotype were used.

wnt11 nontransgenic embryos that originated from the same transgenic mosaic founder fish to minimize genetic background variability in cadherin stainings and to be able to analyze the effects of Wnt11 in a predefined time window at the onset of gastrulation (for details, see [Experimental Procedures](#)). In ectodermal and mesodermal progenitor cells within the germ ring margin of *slb/wnt11* mutant embryos, E-cadherin recognized by specific zebrafish E-cadherin antibodies ([Babb and Marrs, 2004](#)) was predominantly localized to the plasma membrane and in a few cytoplasmic dots ([Figure 3A](#); ratio of plasma membrane/cytoplasmic E-cadherin staining = 1.75 ± 0.25 ; data not shown). In contrast, when Wnt11 expression was induced at the onset of gastrulation in *slb-hs-wnt11-HA* transgenic

embryos, E-cadherin showed irregular plasma membrane staining and appeared in more cytoplasmic dots ([Figure 3D](#); ratio of plasma membrane/cytoplasmic E-cadherin staining = 1.66 ± 0.23 ; $p < 0.001$). This indicates that Wnt11 expression leads to changes in the subcellular localization of E-cadherin from the plasma membrane into cytoplasmic dots. Importantly, the differences in E-cadherin subcellular distribution were not accompanied by recognizable changes in the overall expression levels of E-cadherin (data not shown), nor did they lead to recognizable changes in the intracellular localization of other membrane-associated proteins such as GAP43-GFP and Strabismus-HA (for differences in ratio of plasma membrane/cytoplasmic staining, $p > 0.05$ for both GAP43-GFP and Strabismus-HA; [Figure S1](#)).

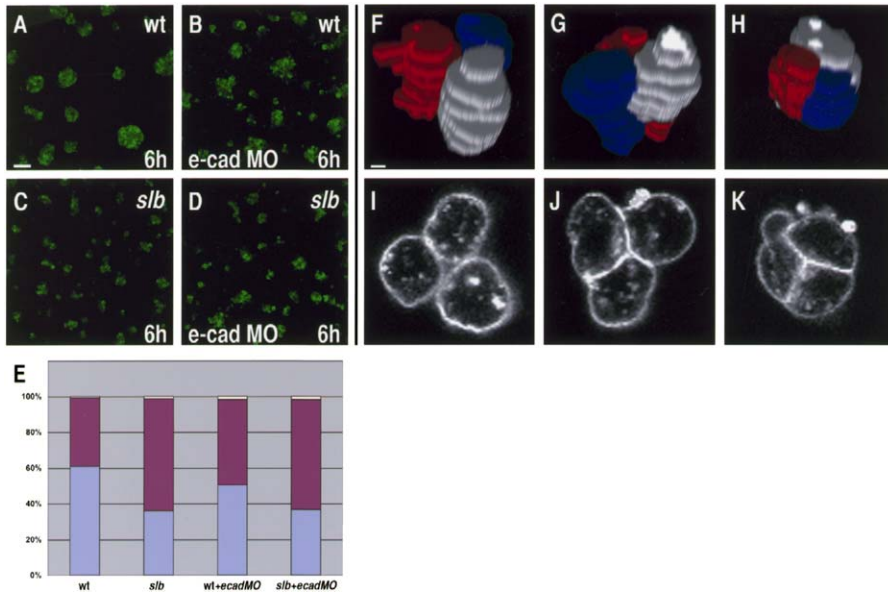


Figure 2. Cohesion between Mesendodermal Cells in Culture
(A–D) Confocal images of primary mesendodermal progenitors labeled with GAP43-GFP from wild-type (A and B) and *slb/wnt11* mutant embryos (C and D) plated on fibronectin after 6 hr in culture either uninjected (A and C) or injected with 8 ng of *e-cadherin-MO* (B and D). The scale bar represents 100 μ m.
(E) Relative amounts of “loose” (nonconfluent, yellow) versus “small” (≤ 10 cells, red) versus “big” (>10 cells, blue) cell aggregates in wild-type and *slb/wnt11* \pm *e-cadherin-MO* cultures after 6 hr. For each condition, 250–500 aggregates from three to four independent experiments were scanned and averaged.
(F–H) Three-dimensional representation of a small mesendodermal cell aggregate shortly after the cells contacted each other (F), 16 min later (G), and after confluency was reached (60 min after initial contact, H). The white and blue cells depicted in (F)–(H) changed their position relative to each other at least once; compare positions in (F) with (G). The scale bar represents 10 μ m.
(F–H) Cross-section through the equatorial region of the cell aggregate shown in (I)–(K) to visualize the contact area between the cells.

Rab5 Function in Wnt11-Mediated E-Cadherin Localization, Mesendodermal Cell Cohesion, and Prechordal Plate Morphogenesis
Questions remain as to the mechanism by which Wnt11 regulates E-cadherin localization. One possible sce-

nario is that Wnt11 induces endocytosis and/or recycling of E-cadherin as a mechanism to promote cell-cell contact dynamics. To test this hypothesis, we first determined whether the previously described cytoplasmic dots containing E-cadherin are endocytic. To mark

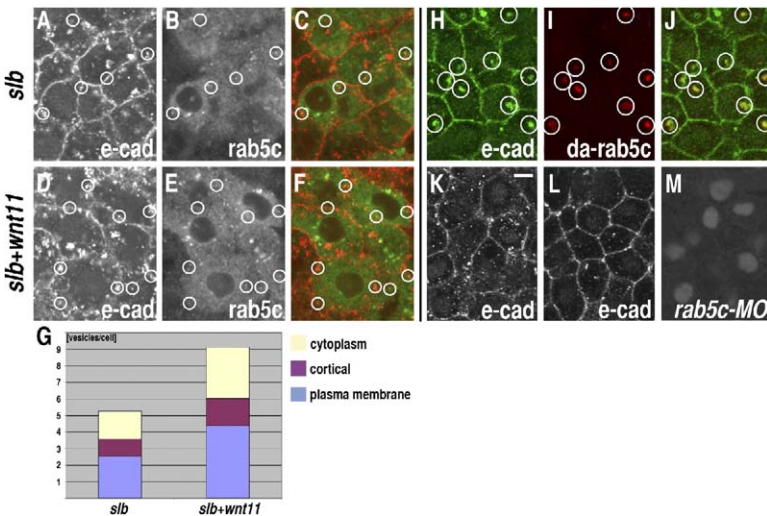


Figure 3. Wnt11 and Rab5c Effects on Subcellular Localization of E-Cadherin within Germ Ring Cells at the Onset of Gastrulation
In all images, confocal sections of shield stage (60% epiboly) epiblast cells at the dorsal region of the germ ring were chosen for analysis (for details, see [Experimental Procedures](#)).
(A–F) Face-on views of epiblast cells in *slb/wnt11* mutant embryos (A–C) and *slb-hs-wnt11-HA* transgenic embryos (D–F) 30 min after the heat shock at shield stage stained with an antibody directed against zebrafish E-cadherin (A and D) and injected with 100 pg *rab5c-YFP* mRNA at dome stage to mark Rab5c-positive early endosomes (B and E). (C and F) Merged picture of (A) and (D) with (B) and (E).
(G) Numbers of E-cadherin/Rab5c-YFP double-positive vesicles overlapping with the plasma membrane (plasma membrane), close (≤ 1 μ m) to the plasma membrane (cortical), and

in the cytoplasm further away (>1 μ m) from the plasma membrane (cytoplasm) in *slb/wnt11* mutant embryos and heat-shocked *slb-hs-wnt11-HA* transgenic embryos. For all categories, significant differences were observed; $p < 0.001$; $n = 88$ cells from 15 embryos for each case.
(H–J) E-cadherin staining (H) and da-Rab5c-YFP (I) in *slb/wnt11* mutant embryo injected with 100 pg *da-rab5c-YFP* mRNA.
(J) Merged picture of (H) and (I).
(K–M) E-cadherin staining in *slb-hs-wnt11-HA* transgenic embryos 30 min after the heat shock either uninjected (K) or injected with 8 ng *rab5c-MO* (L). The scale bar represents 10 μ m. (M) Localization of fluorescein-labeled *rab5c-MO* in (L).

endocytic vesicles, we injected mRNA coding for a YFP-fusion of the zebrafish GTPase Rab5c, a highly conserved key regulator of endocytosis (Zerial and McBride, 2001) that has previously been shown to label endocytic vesicles and early endosomes in gastrulating zebrafish cells (Scholpp and Brand, 2004). When comparing *slb/wnt11* mutant embryos with *slb-hs-wnt11-HA* embryos expressing Wnt11 at the onset of gastrulation, we found that in *slb/wnt11* mutants, 5.25 ± 2.70 E-cadherin-positive dots per cell colocalized with Rab5c (Figures 3A–3C and 3G), while in *slb-hs-wnt11-HA* embryos, the number of colocalizing E-cadherin dots was significantly increased (9.11 ± 4.27 ; $p < 0.001$; Figures 3D–3G). In contrast, the size and/or shape of double-positive vesicles remained unchanged upon expression of Wnt11 in *slb/wnt11* mutant embryos, suggesting that Wnt11 does not interfere with vesicle morphology (Figures 3A–3F; data not shown). This indicates that Wnt11 expression leads to an increase in the proportion of Rab5c-positive endocytic E-cadherin vesicles.

To determine whether Rab5 is involved in Wnt11-mediated endocytosis of E-cadherin, we first activated Rab5c-mediated endocytosis in *slb/wnt11* mutants by overexpressing an activated form of *rab5c* (*da-rab5c*; for details, see Experimental Procedures; Pelkmans et al., 2004). When *da-rab5c-YFP* mRNA was overexpressed in *slb/wnt11* mutant embryos, the amount of double-positive vesicles per cell was increased 3.70 ± 2.15 times compared to *slb/wnt11* mutant embryos injected with *rab5c-YFP* mRNA ($p < 0.001$; $n = 60$ cells from 10 embryos; Figures 3H–3J), suggesting that Rab5c is able to promote E-cadherin endocytosis in *slb/wnt11* mutant embryos. In addition, the fluorescence intensity sum of double-positive vesicles significantly increased in *slb/wnt11* mutant embryos overexpressing *da-rab5c-YFP* as compared to nonexpressing *slb/wnt11* control embryos ($p < 0.001$; data not shown), indicating that *da-Rab5c* promotes both number and intensity of E-cadherin/Rab5c double-positive vesicles. We next tested whether inhibiting Rab5c-mediated endocytosis blocks the previously observed Wnt11-mediated decrease in the ratio of membrane-bound to cytoplasmic E-cadherin staining. Injecting *slb-hs-wnt11-HA* embryos expressing Wnt11 at the onset of gastrulation with *rab5c-MO* (for details, see Experimental Procedures) efficiently blocked the decrease in the ratio of membrane-bound to cytoplasmic E-cadherin staining previously observed in these embryos (ratio of plasma membrane/cytoplasmic E-cadherin staining = 1.70 ± 0.21 in uninjected *slb-hs-wnt11-HA* embryos versus 1.86 ± 0.25 in *slb-hs-wnt11-HA* embryos injected with 8 ng *rab5c-MO*; $p < 0.01$; $n = 42$ cells from 7 embryos; Figures 3K–3M). These data indicate that Rab5c can function as a mediator of Wnt11 in regulating E-cadherin endocytosis.

To further address whether Rab5c can also function as a mediator of Wnt11 modulating mesendodermal cell cohesion in culture, we tested both whether knocking down Rab5c activity in wild-type cells leads to a similar aggregation phenotype as previously observed with *slb/wnt11* mutant cells and whether activating Rab5c in *slb/wnt11* cells can rescue the mutant phenotype. When *rab5c-MO* was expressed in mesendodermal cells, the relative amount of nonconfluent aggregates

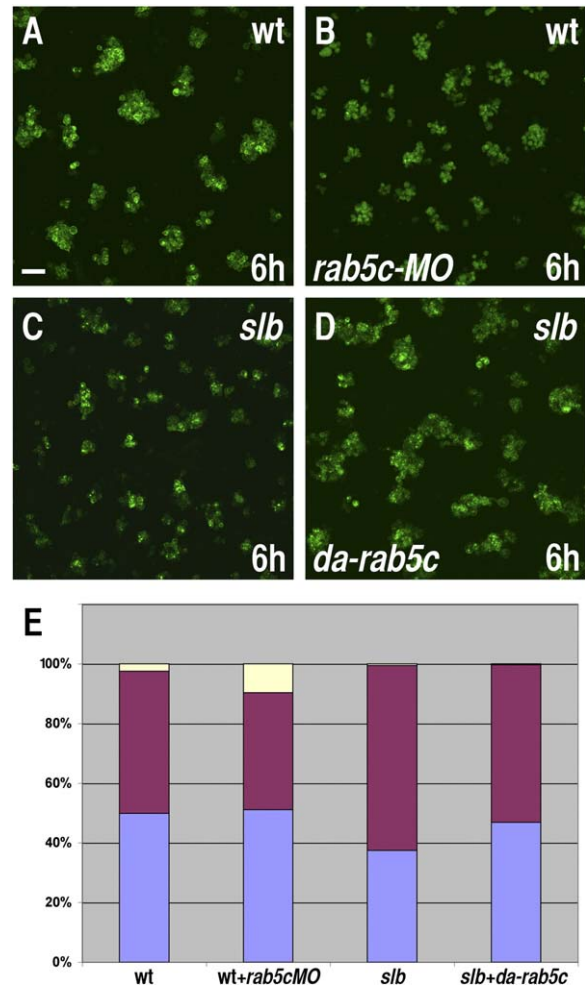


Figure 4. Rab5c Function in Mesendodermal Cell Cohesion
(A–D) Confocal images of primary mesendodermal progenitors labeled with GAP43-GFP from wild-type (A and B) and *slb/wnt11* mutant embryos (C and D) plated on fibronectin after 6 hr in culture either uninjected (A and C) or injected with 8 ng *rab5c-MO* (B) or 100 pg *da-rab5c* mRNA (D). The scale bar represents 100 μ m. (E) Ratios of “loose” (nonconfluent, yellow) versus “small” (≤ 10 cells, red) versus “big” (>10 cells, blue) cell aggregates in wild-type \pm *rab5c-MO* and *slb/wnt11* \pm *da-rab5c* mRNA cultures after 6 hr. For each condition, 650–2400 aggregates from 5–10 independent experiments were scanned and averaged.

was significantly increased, while the fraction of small confluent aggregates was significantly decreased as compared to untreated wild-type controls ($p < 0.01$; Figures 4A, 4B, and 4E). Conversely, expressing *da-Rab5c* in *slb/wnt11* mutant cells significantly increased the fraction of large confluent aggregates at the expense of small confluent aggregates as compared to uninjected *slb/wnt11* cells ($p < 0.001$; Figures 4C–4E). These findings indicate that Rab5c can function as a mediator of Wnt11 in regulating mesendodermal cell cohesion in culture.

To determine whether Rab5c can also interfere with Wnt11-mediated tissue morphogenesis in vivo, we tested whether the *slb/wnt11* prechordal plate movement defect can be phenocopied and rescued by manipulating Rab5c activity. Wild-type embryos injected

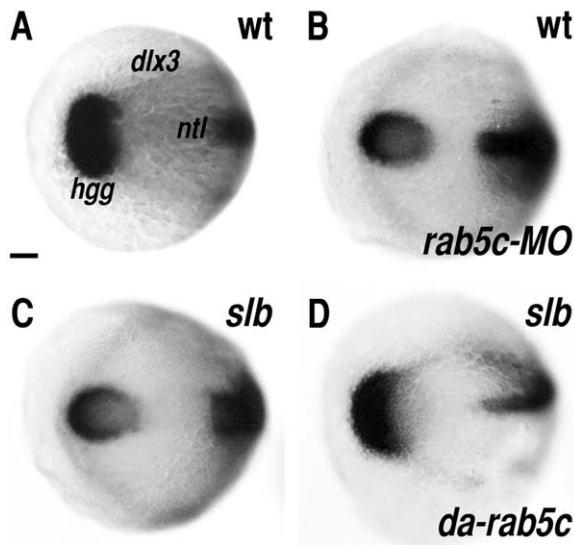


Figure 5. Rab5c Function in Prechordal Plate Morphogenesis

Position of the prechordal plate stained for *hgg1* relative to the anterior edge of the neural plate marked with *dlx3* and the notochord anlage expressing *ntl* at bud stage in a wild-type control embryo (A), a wild-type embryo injected with 8 ng *rab5c-MO* (B), an *slb/wnt11* mutant embryo (C), and an *slb/wnt11* mutant injected with 100 pg *da-rab5c-YFP* mRNA (D). Dorsal views with anterior to the left. The scale bar represents 50 μ m.

with *rab5c-MO* frequently showed a posteriorly displaced and elongated prechordal plate at the end of gastrulation, thus phenocopying the *slb/wnt11* mutant phenotype (Figures 5A and 5B; Table 1), while *slb/wnt11* mutant embryos expressing *da-rab5c-YFP* frequently formed a prechordal plate that was wild-type in appearance, indicating a rescue of the mutant phenotype (Figures 5C and 5D; Table 1). Injecting either a dominant-negative form of *dynamain2* (*dn-dyn*; for details, see Experimental Procedures) or *RN-tre* mRNA, two known inhibitors of Rab5- and Clathrin-mediated endocytosis (Scholpp and Brand, 2004), had similar, but also slightly weaker, effects than *rab5c-MO* (data not shown; Table 1), supporting the notion that Rab5c is required for normal prechordal plate morphogenesis. Importantly, previously described expression of *da-*

rab5c-, *dn-dyn-*, and *RN-tre* mRNA or *rab5c-MO* (Table 1) did not lead to any evident changes in patterning of the gastrula as monitored by the expression of various marker genes for dorsoventral patterning and mesendodermal induction in the injected embryos (Figure S2). Furthermore, although we observed consistent and reproducible phenocopy/rescue of the prechordal plate phenotype by modulating Rab5c activity, we were unable to influence the *slb/wnt11* notochord phenotype, suggesting that the notochord is less sensitive to changes in Rab5c activity (Table S1). Taken together, these data indicate that Rab5c can function as a mediator of Wnt11 to determine prechordal plate morphogenesis during gastrulation.

Wnt11 and Rab5 Function in Adhesion of Mesendodermal Cells to E-Cadherin

The observations that Wnt11 and Rab5c affect the subcellular localization of E-cadherin together with prechordal plate progenitor cell cohesion and migration suggest that Wnt11 and Rab5c control cell cohesion and migration by modulating E-cadherin adhesiveness. In order to directly test whether Wnt11 and Rab5c are required for proper adhesion of mesendodermal cells to E-cadherin, we used atomic force microscopy (AFM) to measure the specific de-adhesion forces needed to separate single mesendodermal cells from substrates decorated with E-cadherin. We have previously described the use of AFM for measuring adhesion forces of single cells from zebrafish gastrula stage embryos to substrates decorated with fibronectin (Puech et al., 2005). In short, we prepared cultures of single mesendodermal cells, and coupled one single cell to the cantilever of the AFM microscope by coating the cantilever with the lectin ConA, which strongly binds zebrafish gastrulating cells (Puech et al., 2005). We then tested this cell probe on E-cadherin-decorated substrates by first pressing the cell on the substrate for various contact times and then pulling it away from the substrate and recording the de-adhesion forces needed to completely dissociate the cell from the substrate (Figure 6A; for details, see Experimental Procedures). The specificity of our measurements was determined by knocking down E-cadherin in mesendodermal cells and adding EGTA and indole-3-acetic acid (IAA) to the culture medium to inhibit cadherin binding (Figure 6B).

Table 1. Rab5c Function in Prechordal Plate Morphogenesis

Injected	Genotype	Wild-Type (%)	<i>slb</i> (%)	Abnormal (%)	Total (n)
-	wt	100	0	0	72
<i>rab5c-MO</i>	wt	43	51	6	120
<i>RNtre</i>	wt	69	29	2	51
<i>dn-dyn</i>	wt	75	25	0	55
<i>GFP</i>	<i>slb/wnt11</i>	4	96	0	48
<i>da-rab5c</i>	<i>slb/wnt11</i>	40	60	0	58
<i>heat-shock</i>	<i>slb/wnt11</i>	9	91	0	99
<i>heat-shock</i>	<i>slb-hs-wnt11-HA</i>	76	24	0	87

Eight nanograms of *rab5c-morpholino* (*MO*) and 200 pg, 100 pg, and 100 pg of *RNtre*, cytoplasmic *GFP*, and *da-rab5c* mRNA, respectively, were injected into one-cell stage embryos; 50 pg *dn-dyn* mRNA was injected into one- to two-cell stage embryos. *slb-hs-wnt11-HA* and *slb/wnt11* nontransgenic control embryos were heat-shocked at early shield stage for 20 min at 39°C (for details, see Experimental Procedures). Embryos classified as “*slb*” displayed an elongated, posteriorly displaced prechordal plate at the end of gastrulation (bud stage), and embryos classified as “abnormal” showed other variable defects in morphogenesis of prechordal plate and notochord.

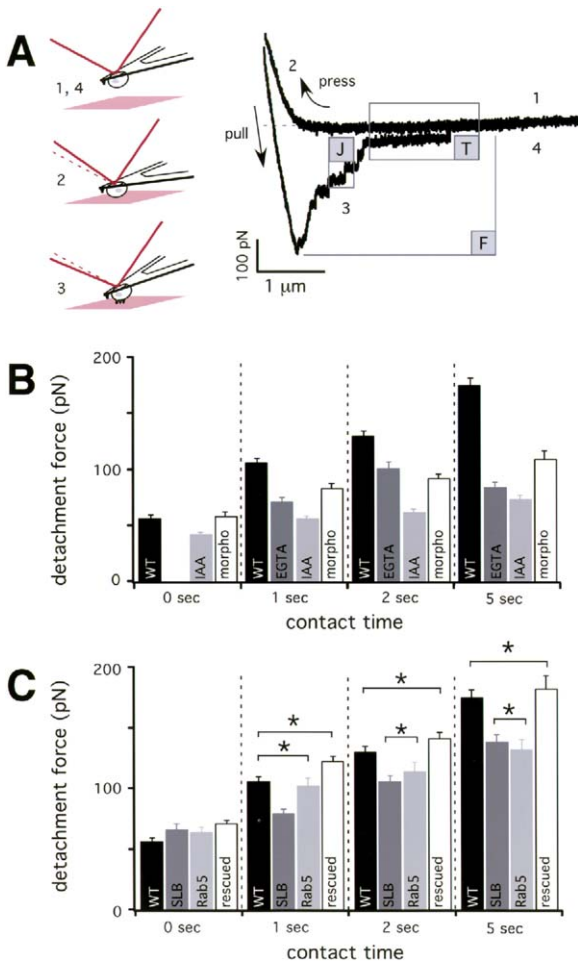


Figure 6. Measurements of De-adhesion Forces of Single Mesodermal Cells to Substrates Decorated with E-Cadherin

(A) Schematic of an AFM single cell adhesion experiment on a decorated surface and typical force curves showing the de-adhesion events. A single cell is captured using a lectin-decorated cantilever (1) and then pressed on a cadherin-decorated substrate (2). After a prescribed contact time, the cell/cantilever is separated from the substrate at a controlled speed (3). The force curve shows a maximal detachment force jump (F), with several small unbinding events either preceded (T) or not preceded (J) by a force plateau. In the end, the cell/cantilever and the substrate are fully separated (4).

(B and C) Histograms of maximal detachment force for different conditions, cell types, and contact times.

(B) Control experiments showing wild-type cells (WT) in the presence of either EGTA to remove Ca^{2+} or IAA to compete with E-cadherin binding and wild-type cells injected with *e-cadherin-MO* (morpho) to reduce E-cadherin activity.

(C) Comparison of the de-adhesion forces measured for wild-type (WT) and *slb/wnt11* mutant (SLB) cells, wild-type cells injected with *rab5c-MO* (rab5), and *slb/wnt11* mutant cells expressing 10 pg *slb/wnt11* mRNA (rescued) for contact times ranging from 0 to 5 s. Asterisks indicate values that are not significantly different ($p > 0.05$). The data are presented as mean \pm SEM.

We observed a significant decrease in the de-adhesion forces needed to dissociate wild-type versus *slb/wnt11* mutant cells from E-cadherin substrates for contact times ranging from 1 to 5 s, suggesting that Wnt11 is required for proper adhesion of mesodermal cells to E-cadherin (Figure 6C). This reduction of de-adhe-

sion forces in *slb/wnt11* mutant embryos was completely rescued by expressing low amounts of *slb/wnt11* mRNA (10 pg/embryo) in mutant cells (Figure 6C), supporting the specificity of the observed phenotype. Similarly, there was a significant decrease in the de-adhesion forces measured for dissociation of wild-type versus *rab5c-MO*-expressing cells for contact times ranging from 1 to 5 s, indicating that Rab5c is also needed for adhesion of mesodermal cells to E-cadherin (Figure 6C). Taken together, these data provide evidence that Wnt11 and Rab5c are needed for proper adhesion of mesodermal cells to E-cadherin, thereby supporting our hypothesis that Wnt11 and Rab5c modulate cell cohesion and tissue morphogenesis through E-cadherin.

Discussion

We provide evidence that Rab5c mediates Wnt11 control of mesodermal cell cohesion and migration. Furthermore, we show that Wnt11 and Rab5c regulate the endocytosis of E-cadherin and are both required for E-cadherin-mediated cohesion of mesodermal cells. These results suggest that Wnt11 controls prechordal plate progenitor migration by modulating E-cadherin-mediated cell cohesion through Rab5c, a novel mechanism by which Wnt11 functions in gastrulation.

Our previous findings demonstrated that in zebrafish, prechordal plate progenitors, after internalizing at the germ ring margin, exhibit active migratory behavior toward the animal pole of the gastrula using the overlying ectoderm as a substrate on which to migrate (Montero and Heisenberg, 2004). Furthermore, we found that Wnt11 and E-cadherin are involved in this process (Montero et al., 2005; Ulrich et al., 2003). Wnt11 controls the speed and direction of prechordal plate progenitor migration at the onset of gastrulation, possibly by aligning the orientation of cellular processes to the direction of individual cell movement (Ulrich et al., 2003). E-cadherin is required for prechordal plate progenitor spreading at the interface between mesoderm and ectoderm and subsequent migration during later stages of gastrulation (Babb and Marris, 2004; Montero et al., 2005; Shimizu et al., 2005). This suggests that Wnt11 and E-cadherin play similar roles in that they both control prechordal plate cell migration and process formation. However, Wnt11 predominantly functions within the prechordal plate while E-cadherin appears to have multiple and diverse functions in controlling cell movements and rearrangements within both the forming prechordal plate and overlying ectodermal germ layer (Babb and Marris, 2004; Kane et al., 2005; Montero et al., 2005; Shimizu et al., 2005).

We now show that Wnt11 and E-cadherin functionally interact during zebrafish gastrulation and that Rab5, a key component in the regulation of intracellular trafficking both at the level of receptor endocytosis and endosome dynamics (Zerial and McBride, 2001), is involved in this process. There are different possibilities of how Wnt11 controls E-cadherin activity through Rab5. One possibility is that Wnt11 promotes Rab5c-mediated endocytosis and recycling of E-cadherin to regulate the dynamics of E-cadherin turnover at the plasma mem-

brane. Alternatively, Wnt11 might regulate Rab5-dependent actin remodeling, which secondarily could affect the adhesive and cohesive properties of mesendodermal cells. The observation from this study, that E-cadherin is endocytosed in response to Wnt11 and Rab5c, suggests that Wnt11 modulates E-cadherin dynamics through endocytosis and recycling.

We further propose in this study that a Wnt11-mediated increase in cadherin dynamics regulates the cohesive and migratory activity of mesendodermal progenitors. For a group of cells to adhere and rearrange into coherent clusters, they must not only be able to stick to each other but also to dynamically disassemble and reassemble adhesion complexes. This becomes even more important for migrating cells that need to rapidly de-adhere and re-adhere in order to translocate over their substrate. Endocytosis and recycling of adhesion molecules, including E-cadherin, are likely to be involved in these processes as they represent key components for junction formation and remodeling (Le et al., 1999) and are associated with cell migration (Fujita et al., 2002). In *Drosophila* oogenesis, the level of DE-cadherin expression determines intercellular motility, suggesting that synthesis and turnover of DE-cadherin regulate cell migration (Niewiadomska et al., 1999). It is therefore conceivable that Wnt11 promotes the ability of mesendodermal cells to dynamically build up and disassemble E-cadherin-based cell-cell junctions required for effective cell cohesion and migration.

Interestingly, prechordal plate progenitors move as a cohesive group of cells toward the animal pole, with single prechordal plate progenitor cells following highly aligned movement tracks (Montero et al., 2005; Ulrich et al., 2003). The cohesive character of prechordal plate progenitors is likely to influence how well the movement tracks of individual progenitor cells are aligned to each other. Our observations that Wnt11 is required for both prechordal plate progenitor cohesion and the coherent migration of single mesendodermal progenitors in vivo suggest that Wnt11 controls “movement coherence” of prechordal plate progenitors by promoting cohesion between these cells. Consistent with this idea, prechordal plate progenitors move considerably faster toward the animal pole than the more loosely associated mesendodermal progenitors from paraxial regions of the gastrula (unpublished observations), and Wnt11 is predominantly required for prechordal plate but not paraxial mesendodermal cell migration (Heisenberg et al., 2000; Kilian et al., 2003). This points to the interesting possibility that Wnt11 function becomes predominantly visible in prechordal plate progenitors because these cells particularly depend on cohesion for efficient migration.

We also suggest in this study that E-cadherin functions as one target molecule through which Wnt11 controls prechordal plate progenitor migration during gastrulation. Previous work has shown that E-cadherin is the prime classical cadherin expressed at the onset of zebrafish gastrulation, and that it is required for mesendodermal cell cohesion and migration (Babb and MARRS, 2004; Kane et al., 2005; Montero et al., 2005; Shimizu et al., 2005). These data, in combination with our findings that E-cadherin is required downstream of Wnt11 and that both Wnt11 and Rab5c can modulate the intra-

cellular localization and adhesive activity of E-cadherin, suggest a role for E-cadherin in mediating Wnt11 function. However, it is unlikely that E-cadherin will be the sole target of Wnt11 function in cell cohesion and migration. In fact, the observation from this study that E-cadherin is partially, but not exclusively required for Wnt11 control of mesendodermal cell cohesion, together with our recent finding that Wnt11 modulates the adhesion of mesendodermal cells to fibronectin (Puech et al., 2005), indicate that other adhesion molecules such as integrins must also be involved.

Interestingly, recent findings show that the PCP pathway controls the dynamic modulation of adhesion contacts during *Drosophila* imaginal disc development by regulating endocytosis and/or recycling of E-cadherin adhesion complexes (A. Classen and S. Eaton, personal communication). Considering that several zebrafish homologs of the *Drosophila* PCP pathway also genetically interact with and/or are part of the Wnt11 signaling pathway during gastrulation (Tada et al., 2002; Veeman et al., 2003), this raises the intriguing possibility that Wnt/Fz-mediated E-cadherin endocytosis might represent an evolutionarily conserved mechanism by which tissue morphogenesis is controlled in both vertebrates and invertebrates. Future studies are necessary to reveal possible conserved molecular control mechanisms by which Wnt/Fz signaling regulates E-cadherin endocytosis and the specific contribution of this process for tissue morphogenesis.

Experimental Procedures

Embryo Maintenance

Fish maintenance and embryo collection was carried out as described (Westerfield, 2000). To reduce genetic background variability in our mutant analysis, we only compared homozygous *slb/wnt11^{tx226}* carriers either with TL wild-type fish (cell cohesion and movement assays) or with *slb/wnt11^{tx226} hs-wnt11-HA* transgenic carriers that originated from the same transgenic mosaic founder fish (E-cadherin antibody stainings).

RNA and Morpholino Injection

For mRNA synthesis, cDNAs for cytosolic GFP, GAP43-GFP (Okada et al., 1999), Cyclops (Rebagliati et al., 1998), Wnt11 (Heisenberg et al., 2000), Stbm-HA (Jessen et al., 2002), Rab5c-YFP (Scholpp and Brand, 2004), Rab5c (Q81L)-YFP (*da-rab5c*), RN-tre, and Dynamin2 (K44A) (*dn-dyn*) (Scholpp and Brand, 2004) were used. *Rab5c (Q81L)-YFP* cDNA was directly made from wild-type *Rab5c-YFP* cDNA by site-directed mutagenesis using the primers 5'-CAC GGC CGG ACT GGA GCG GTA TCA C-3' and 5'-GTG ATA CCG CTC CAG TCC GGC CGT G-3'. mRNA and morpholino oligonucleotides (MO) were injected as previously described (Montero et al., 2005); for live time lapse analysis, a 3:1 mixture of *GAP43-GFP* and cytosolic *GFP* mRNAs was used. The amount of *rab5c-YFP* mRNA injected (100 pg/embryo) in the colocalization experiments did not cause any recognizable gain-of-function phenotype at the end of gastrulation (data not shown). The *e-cadherin-MO* has been described elsewhere (Babb and MARRS, 2004; Montero et al., 2005). The fluorescein-coupled *rab5c-MO* (5'-CGCTGGTCCACCTCGC CCGCCATG-3') was directed against the 5'-UTR and tested for specificity by coinjection with *da-rab5c-YFP* mRNA, which efficiently rescued the morphant phenotype (data not shown). Throughout this study, we exclusively used *rab5c*, given that only *rab5c*, but not *rab5a* and *rab5b*, was both expressed during gastrulation and showed a clearly recognizable gastrulation phenotype when “knocked down” (data not shown).

Antibody and In Situ Staining

Antibody and in situ stainings were performed as previously described (Montero et al., 2005; Ulrich et al., 2003). In situ probes

were synthesized from cDNA for *hgg1*, *dlx3*, and *ntl* (Akimenko et al., 1994; Schulte-Merker et al., 1994; Thisse et al., 1994), using a DIG RNA labeling kit (Roche, Mannheim, Germany). The following primary antibodies were used: E-cadherin, polyclonal rabbit (Babb and Marrs, 2004), 1:750/10,000 (whole-mount/Western blotting); HA, monoclonal rat (Roche, Mannheim, Germany), 1:1,000. As secondary antibodies, we used Cy5-coupled anti-rabbit IgG (Jackson Immunolabs, Cambridgeshire, UK), 1:1,000; Alexa-633-coupled anti-rat IgG (Molecular Probes, Karlsruhe, Germany), 1:1,000; HRP-coupled anti-rabbit IgG (Jackson Immunolabs.), 1:10,000.

Image Acquisition and Quantification

Live time lapse imaging was performed as previously described (Ulrich et al., 2003). Immunostained embryos were mounted on agarose-coated dishes in PBS with 0.1% Tween-20, 0.05% Triton X-100 medium with the dorsal side facing up, and images were acquired with a 488, 543, and/or 633 nm laser line on a Zeiss LSM (Carl Zeiss, Jena, Germany) or Leica TCS-SP2 (Bernaheim, Germany) microscope. All confocal images were analyzed and quantified using Volocity 3.0 (Improvision, Coventry, UK), ImageJ v. 1.29–1.32 (<http://rsb.info.nih.gov/ij/>) and Matlab (Mathworks, Natick, MA). The membrane-to-cytosol ratio was calculated on single z-planes using ImageJ by dividing the average staining intensity at the plasma membrane by the average staining intensity within the cytoplasm (excluding the nucleus). For colocalization experiments, double-positive vesicles were only counted when they showed clear overlap and similar morphology. We exclusively analyzed epiblast cells because epiblast and hypoblast cells exhibited a very similar pattern of E-cadherin localization, but epiblast cells were more superficially located within the germ ring and therefore easier to image and quantify (data not shown). Confocal sections were scanned with gain and offset of the photomultiplier tubes set below saturation. The signal intensity for injected rab5c-YFP was set to achieve an optimal signal-to-noise ratio between rab5c-positive vesicles and cytoplasmic background staining. To analyze significance, p values were determined in Microsoft Excel using an unpaired t test with a two-tailed distribution.

Generation of Transgenic Lines

Linearized *hs-wnt11-HA* and GFP constructs were purified with the QIAquick PCR Purification kit (Qiagen, Hilden, Germany) and dialyzed overnight against 0.5x Tris-EDTA buffer. Two hundred fifty picograms of each construct was coinjected into early one-cell stage embryos of homozygous *slb/wnt11* fish as previously described (Gilmour et al., 2002). The *slb-hs-wnt11-HA* transgenic founder line was identified on the basis of GFP expression of the progeny and the F1 generation was screened by Western blotting and whole-mount staining using α -HA antibodies. Experiments were performed with progenies of homozygous transgene carriers of the F2 generation. For heat-shock experiments, homozygous *slb-hs-wnt11-HA* carriers were heat-shocked for 20 min in 39°C, left for 30 min at 28°C, and then fixed for further processing. With this regime, we were able to detect strong Wnt-HA expression (Figure S3) and to efficiently rescue the *slb/wnt11* mutant phenotype at the end of gastrulation (Table 1).

Cell Culture

Cell culture was done as previously described (Montero et al., 2003); for functional tests, 10 pg *wnt11* mRNA, 100 pg *da-rab5c* mRNA, 8 ng *e-cadherin-MO*, or 8 ng *rab5c-MO* were coinjected with 100 pg *cyclops* mRNA; for confocal imaging, an additional 75 pg *GAP43-GFP* mRNA was injected into the embryos. Dissociated cells were adjusted to a concentration of 2×10^5 cells/ml. One hundred microliters of the cell suspension was plated on plastic wells coated with 35.4 ng fibronectin/mm², an abundant extracellular matrix component in *Xenopus* and zebrafish (Marsden and DeSimone, 2003; Trinh and Stainier, 2004). Cells were kept for 6 hr at 25°C and 2% CO₂.

AFM Setup

We used a JPK Nanowizard atomic force microscope (JPK Instruments, Berlin, Germany) on top of an Axiovert 200 inverted microscope (Carl Zeiss, Jena, Germany). The AFM has a linearized piezo

electric ceramic with a 15 μ m range and an infrared laser. We used 320 μ m long cantilevers, with a nominal spring constant of 10 pN/nm (Microlevers, MLCT-AUHW, Veeco, Mannheim, Germany). We calibrated sensibility and spring constant of each cantilever prior to each experiment using built-in routines of the JPK software.

Cantilever and Surface Decoration (AFM)

Cantilevers were plasma cleaned using residual air plasma. They were then functionalized using biotinylated BSA, and incubated in streptavidin and biotinylated ConA. Cantilevers were always kept wet to ensure the integrity of the surface (Puech et al., 2005). Clean glass slides were plasma activated for 1 min and then incubated overnight at 37°C with 0.5 mg/ml biotinylated BSA in 100 mM NaHCO₃ buffer (pH 8.6), 45 min with 0.5 mg/ml streptavidin in PBS, 1 hr with 0.5 mg/ml biotinylated protein A, and finally 3 hr with 50 μ g/ml Fc-tagged E-cadherin from mouse in PBS with 5 mM EGTA. In between steps, surfaces were extensively washed using the buffer used in the next incubation. Prior to use, the nonbound proteins were removed by extensive washing, first with PBS/CaMg, then with fresh DMEM. All chemicals were obtained from Sigma-Aldrich (Steinheim, Germany).

Cell Capture, Adhesion Experiment, and Data Processing (AFM)

Single cells plated on cadherin surfaces were captured as previously described (Puech et al., 2005) using a ConA-decorated cantilever. The cell-cantilever couple was then lifted from the surface (several tens of μ m) and the cell was allowed to establish a firm adhesion on the lever for about 5 to 10 min. After this, the approach and retraction speeds were set to 3.7 μ m/s, the pulling range to 4.5 μ m, the contact time between 0 and 5 s, and the contact force to \sim 300 pN. The complete procedure is summarized in Figure 6A. Five to seven force curves were acquired for each cell for a given contact time, and the cell was subsequently allowed to recover far from the surface for several minutes, before testing a different spot on the surface and/or different contact times. No separation of the captured cell from the cantilever was observed during the pulling experiments, in agreement with previously published results (Wojcikiewicz et al., 2004). Several tens of force curves were acquired per cell and forces did not show clear tendencies depending on the substrate spot tested. To extract the relevant parameters along the retrace curves (Figure 6A), postprocessing with home-programmed procedures using Igor Pro 4.09 (Wavemetrics, Lake Oswego, OR) was employed. This software was also used to extract the means and standard deviations of the data sets and we used built-in procedures of KaleidaGraph (Synergy Software, Reading, PA) for running ANOVA-Tukey HSD tests.

IAA and EGTA Controls (AFM)

Cells were incubated 30 min prior to the AFM measurements with 15 mM tryptophan analog indole-3-acetic acid (IAA; Sigma-Aldrich) as previously described (Perret et al., 2002). During all force measurements, the cells were kept in the presence of the blocking molecule.

Calcium suppression experiments were conducted in the presence of 5 mM EGTA.

Supplemental Data

Supplemental Experimental Procedures, figures, table, and movies are available at <http://www.developmentalcell.com/cgi/content/full/9/4/555/DC1/>.

Acknowledgments

We thank A. Oates, M. Zerial, S. Eaton, J. Geiger, M. Koeppen, and L. Rohde for reading earlier versions of this manuscript, J. Marrs and S. Babb for the kind gift of E-cadherin antibody, and S. Scholpp, A. Siekmann, and M. Brand for help with the *rab5c* cloning. We are especially grateful to J. Sanderson, J. Peychl, and K. Anderson for advice with confocal microscopy and to G. Junghanns, E. Lehmann, M. Fischer, and J. Hueckmann for help with the fish care. This work was supported by grants from the Emmy-

Noether-Program of the Deutsche Forschungsgemeinschaft, the Max-Planck-Gesellschaft, and the Humboldt Foundation.

Received: April 12, 2005

Revised: July 25, 2005

Accepted: August 15, 2005

Published: October 3, 2005

References

- Adler, P.N. (2002). Planar signaling and morphogenesis in *Drosophila*. *Dev. Cell* 2, 525–535.
- Akimenko, M.A., Ekker, M., Wegner, J., Lin, W., and Westerfield, M. (1994). Combinatorial expression of three zebrafish genes related to distal-less: part of a homeobox gene code for the head. *J. Neurosci.* 14, 3475–3486.
- Babb, S.G., and MARRS, J.A. (2004). E-cadherin regulates cell movements and tissue formation in early zebrafish embryos. *Dev. Dyn.* 230, 263–277.
- Djiane, A., Riou, J., Umbhauer, M., Boucaut, J., and Shi, D. (2000). Role of frizzled 7 in the regulation of convergent extension movements during gastrulation in *Xenopus laevis*. *Development* 127, 3091–3100.
- Fujita, Y., Krause, G., Scheffner, M., Zechner, D., Leddy, H.E., Behrens, J., Sommer, T., and Birchmeier, W. (2002). Hakai, a c-Cbl-like protein, ubiquitinates and induces endocytosis of the E-cadherin complex. *Nat. Cell Biol.* 4, 222–231.
- Gilmour, D.T., Maischein, H.M., and Nusslein-Volhard, C. (2002). Migration and function of a glial subtype in the vertebrate peripheral nervous system. *Neuron* 34, 577–588.
- Heisenberg, C.P., Tada, M., Rauch, G.J., Saude, L., Concha, M.L., Geisler, R., Stemple, D.L., Smith, J.C., and Wilson, S.W. (2000). Silberblick/Wnt11 mediates convergent extension movements during zebrafish gastrulation. *Nature* 405, 76–81.
- Jessen, J.R., Topczewski, J., Bingham, S., Sepich, D.S., Marlow, F., Chandrasekhar, A., and Solnica-Krezel, L. (2002). Zebrafish trilobite identifies new roles for Strabismus in gastrulation and neuronal movements. *Nat. Cell Biol.* 4, 610–615.
- Kane, D.A., McFarland, K.N., and Warga, R.M. (2005). Mutations in half baked/E-cadherin block cell behaviors that are necessary for teleost epiboly. *Development* 132, 1105–1116.
- Kilian, B., Mansukoski, H., Barbosa, F.C., Ulrich, F., Tada, M., and Heisenberg, C.P. (2003). The role of Ppt/Wnt5 in regulating cell shape and movement during zebrafish gastrulation. *Mech. Dev.* 120, 467–476.
- Lauffenburger, D.A., and Horwitz, A.F. (1996). Cell migration: a physically integrated molecular process. *Cell* 84, 359–369.
- Le, T.L., Yap, A.S., and Stow, J.L. (1999). Recycling of E-cadherin: a potential mechanism for regulating cadherin dynamics. *J. Cell Biol.* 146, 219–232.
- Marsden, M., and DeSimone, D.W. (2003). Integrin-ECM interactions regulate cadherin-dependent cell adhesion and are required for convergent extension in *Xenopus*. *Curr. Biol.* 13, 1182–1191.
- Montero, J.A., and Heisenberg, C.P. (2004). Gastrulation dynamics: cells move into focus. *Trends Cell Biol.* 14, 620–627.
- Montero, J.A., Kilian, B., Chan, J., Bayliss, P.E., and Heisenberg, C.P. (2003). Phosphoinositide 3-kinase is required for process outgrowth and cell polarization of gastrulating mesendodermal cells. *Curr. Biol.* 13, 1279–1289.
- Montero, J.A., Carvalho, L., Wilsch-Brauninger, M., Kilian, B., Mustafa, C., and Heisenberg, C.P. (2005). Shield formation at the onset of zebrafish gastrulation. *Development* 132, 1187–1198.
- Murphy, C., Saffrich, R., Grummt, M., Gournier, H., Rybin, V., Rubino, M., Auvinen, P., Lutcke, A., Parton, R.G., and Zerial, M. (1996). Endosome dynamics regulated by a Rho protein. *Nature* 384, 427–432.
- Niewiadomska, P., Godt, D., and Tepass, U. (1999). DE-cadherin is required for intercellular motility during *Drosophila* oogenesis. *J. Cell Biol.* 144, 533–547.
- Okada, A., Lansford, R., Weimann, J.M., Fraser, S.E., and McConnell, S.K. (1999). Imaging cells in the developing nervous system with retrovirus expressing modified green fluorescent protein. *Exp. Neurol.* 156, 394–406.
- Palacios, F., Tushir, J.S., Fujita, Y., and D'Souza-Schorey, C. (2005). Lysosomal targeting of E-cadherin: a unique mechanism for the down-regulation of cell-cell adhesion during epithelial to mesenchymal transitions. *Mol. Cell Biol.* 25, 389–402.
- Pelkmans, L., Burli, T., Zerial, M., and Helenius, A. (2004). Caveolin-stabilized membrane domains as multifunctional transport and sorting devices in endocytic membrane traffic. *Cell* 118, 767–780.
- Perret, E., Benoliel, A.M., Nassoy, P., Pierres, A., Delmas, V., Thiery, J.P., Bongrand, P., and Feracci, H. (2002). Fast dissociation kinetics between individual E-cadherin fragments revealed by flow chamber analysis. *EMBO J.* 21, 2537–2546.
- Puech, P.-H., Taubenberger, A., Ulrich, F., Krieg, M., Muller, D.J., and Heisenberg, C.-P. (2005). Measuring cell adhesion forces of primary gastrulating cells from zebrafish using atomic force microscopy. *J. Cell Sci.*, in press.
- Rebagliati, M.R., Toyama, R., Haffter, P., and Dawid, I.B. (1998). cyclops encodes a nodal-related factor involved in midline signaling. *Proc. Natl. Acad. Sci. USA* 95, 9932–9937.
- Scholpp, S., and Brand, M. (2004). Endocytosis controls spreading and effective signaling range of Fgf8 protein. *Curr. Biol.* 14, 1834–1841.
- Schulte-Merker, S., van Eeden, F.J., Halpern, M.E., Kimmel, C.B., and Nusslein-Volhard, C. (1994). no tail (ntl) is the zebrafish homologue of the mouse T (Brachyury) gene. *Development* 120, 1009–1015.
- Shimizu, T., Yabe, T., Muraoka, O., Yonemura, S., Aramaki, S., Hatta, K., Bae, Y.K., Nojima, H., and Hibi, M. (2005). E-cadherin is required for gastrulation cell movements in zebrafish. *Mech. Dev.* 122, 747–763.
- Spaargaren, M., and Bos, J.L. (1999). Rab5 induces Rac-independent lamellipodia formation and cell migration. *Mol. Biol. Cell* 10, 3239–3250.
- Stern, C. (2004). *Gastrulation: From Cells to Embryo* (Cold Spring Harbor, NY: Cold Spring Harbor Laboratory Press).
- Tada, M., Concha, M.L., and Heisenberg, C.P. (2002). Non-canonical Wnt signalling and regulation of gastrulation movements. *Semin. Cell Dev. Biol.* 13, 251–260.
- Thisse, C., Thisse, B., Halpern, M.E., and Postlethwait, J.H. (1994). Goosecoid expression in neurectoderm and mesendoderm is disrupted in zebrafish cyclops gastrulas. *Dev. Biol.* 164, 420–429.
- Trinh, L.A., and Stainier, D.Y. (2004). Fibronectin regulates epithelial organization during myocardial migration in zebrafish. *Dev. Cell* 6, 371–382.
- Ulrich, F., Concha, M.L., Heid, P.J., Voss, E., Witzel, S., Roehl, H., Tada, M., Wilson, S.W., Adams, R.J., Soll, D.R., and Heisenberg, C.P. (2003). Slb/Wnt11 controls hypoblast cell migration and morphogenesis at the onset of zebrafish gastrulation. *Development* 130, 5375–5384.
- Veeman, M.T., Axelrod, J.D., and Moon, R.T. (2003). A second canon. Functions and mechanisms of β -catenin-independent Wnt signaling. *Dev. Cell* 5, 367–377.
- Warga, R.M., and Kimmel, C.B. (1990). Cell movements during epiboly and gastrulation in zebrafish. *Development* 108, 569–580.
- Westerfield, M. (2000). *The Zebrafish Book*, Fourth Edition (Eugene: University of Oregon Press).
- Winklbauer, R., Medina, A., Swain, R.K., and Steinbeisser, H. (2001). Frizzled-7 signalling controls tissue separation during *Xenopus* gastrulation. *Nature* 413, 856–860.
- Wojcikiewicz, E.P., Zhang, X., and Moy, V.T. (2004). Force and compliance measurements on living cells using atomic force microscopy (AFM). *Biol. Proced. Online* 6, 1–9.
- Zerial, M., and McBride, H. (2001). Rab proteins as membrane organizers. *Nat. Rev. Mol. Cell Biol.* 2, 107–117.